Dalton Transactions

Accepted Manuscript

ROYAL SOCIETY OF CHEMISTRY

www.rsc.org/dalton

Journal Name

RSCPublishing

ARTICLE

Weak aurophilic interactions in a series of Au(III) double salts

Cite this: DOI: 10.1039/x0xx00000x

Alexander N. Chernyshev,[a,b] Maria V. Chernysheva,[a] Pipsa Hirva,[c] Vadim Yu. Kukushkin,[b] and Matti Haukka*[,a]

Received 00th January 2012,
Accepted 00th January 2012

DOI: 10.1039/x0xx00000x

www.rsc.org/

In this work, several new examples of rare $Au^{III}\cdots Au^{III}$ aurophilic contacts are reported. A series of gold(III) double salts and complexes, *viz.* $[AuX_2(L)][AuX_4]$ (L = 2,2′-bipyridyl, X = Cl **1**, Br **2**; L = 2,2′-bipyrimidine, X = Cl **3**, Br **4**; L = 2,2′-dipyridylamine, X = Cl **5**, Br **6**), $[AuX_3(biq)]$ (biq = 2,2′-biquinoline, X = Cl **7**, Br **8**), $[LH][AuX_4]$ (L = 2,2′-bipyridyl, X = Cl **9**; L = 2,2′-bipyrimidine, X = Cl **12**; L = 2,2′-dipyridylamine, X = Cl **14**, Br **15**; L = 2,2′-biquinoline, X = Cl **17**, Br **18**), $[AuBr_2(bpy)]_2[AuBr_4][AuBr_2]$ **10**, $[AuCl_2(bpm)][AuCl_2]$ **11**, $(bpmH)_2[AuBr_4][AuBr_2]$ **13**, and (dpaH)$[AuBr_2]$ **16** (**1**, **2**, and **7** were reported earlier) was synthesized by coordination of a particular ligand to Au^{III} center and subsequent reduction of the formed product with acetone. Inspection of X-ray structural data for **1**, **3**–**6**, and **11** indicate that the Au^{III} metal centers approach each other closer than the sum of their van der Waals radii, thus forming the aurophilic contacts, which were confirmed by topological charge density analysis according to the Quantum Theory of Atoms in Molecules (QTAIM). In **1**, **4**, and **11**, such contacts are located only between the metal centers of the ion pair, whereas in **3**, the aurophilic interactions form the cation-anion-anion array, and in **5**, the aurophilicity exists between the gold atoms of the cations. It was also demonstrated that the interatomic distance alone is not a reliable measure of the aurophilic interactions, at least at the weakest limit of the interaction strength, and need to be complemented with structural analysis of the whole molecule and computational results.

Introduction

Metallophilic interactions, both ligand-supported and ligand-unsupported, attract enormous interest in organometallic chemistry because they can facilitate an appearance of unusual properties of materials, such as, luminescence,[1–10] magnetism,[11] sensing,[12,13] thermochromism,[14,15] solvatochromism,[16] as well as electrical conductivity.[17–20] The origin of the investigation of metallophilic interactions lies in gold-gold contacts i.e. aurophilic interactions.[21] Such interactions are widely utilized in the gold chemistry due to the steric accessibility of the gold center (gold in its most common oxidation states Au^{I} and Au^{III} exist in sterically nonhindered linear and square planar arrangements, respectively), and the strength of the aurophilic contacts (the energy of the aurophilic contacts is comparable to the energy of hydrogen bonding[22,23]). The strength of aurophilicity is commonly associated with the relativistic effects, which are stronger for gold than for most of the other heavy metals.[22,24–27]

Until the last decade the term "aurophilicity" was almost synonymous to the $Au^{I}\cdots Au^{I}$ interactions. However, in the mid-2000th it was proved theoretically that Au^{III} can also favour an aurophilic attraction.[28,29] Since that time some gold complexes featuring $Au^{III}\cdots Au^{III}$ interactions have been synthesized and characterized.[30–33] However, such compounds, especially those with unsupported aurophilic interactions, are still rather rare.

In the current work, we introduce the syntheses and structural features of a series of new and known gold(III) double salts exhibiting the aurophilic interactions. Our goal was to reveal whether the formation of the aurophilic contact possible at the long gold···gold distances and to study the effect of the overall arrangement of molecules and weak interactions other than aurophilicity on the formation of aurophilic contacts. In order to achieve this goal, we have used a combined approach based on structural analysis of the molecules and topological charge density computations.

Results and discussion

Synthesis of complexes 1–8

Two general synthetic approaches to gold(III) double salts are known. The first one is a metathesis reaction between the salts of gold-containing cations and anions (Scheme 1, route A).[31] The second one is based on the interaction of gold-

containing precursors (AuX_3 or $[AuX_4]^-$, X = Cl, Br) with one half equivalent of a chelating ligand (Scheme 1, route B).[34]

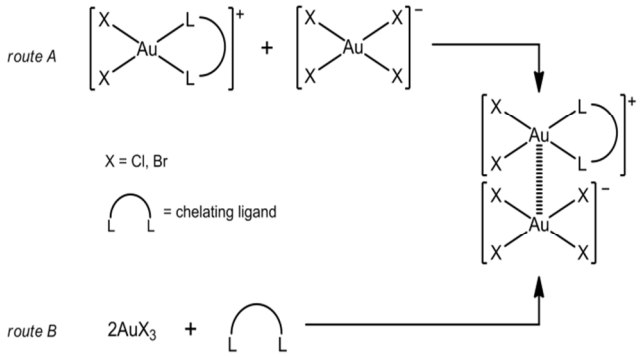

Scheme 1. Two main approaches to gold(III) double salts.

Both methods have their own advantages and disadvantages. The first provide a useful route to double salts with different halides in cation and anion, as well as mixed valence and mixed metal complexes, such as $Au^{III}\cdots Au^{I}$, $Pt^{II}\cdots Au^{III}$, or $Pt^{II}\cdots Au^{I}$ systems.[31,34] However, this approach requires a separate step for preparation of the starting compounds suitable for the metathesis. The second route leads to generation of the double salts with no variation on the halides or metal centers, but it allows simplification of the synthetic procedure by excluding the additional step of preparation of the starting compounds. Owing to this reason we have utilized the second method in the present work.

With the aim to obtain gold(III) complexes featuring the aurophilic interactions, we synthesized a series of double salts **1**–**8** by the reaction of AuX_3 (X = Cl, Br) with several chelating nitrogen-containing ligands, namely 2,2'-bipyridyl (bpy), 2,2'-bipyrimidine (bpm), 2,2'-dipyridylamine (dpa), and 2,2'-biquinoline (biq) (Scheme 2, left). Among the obtained compounds, **1** and **2** were previously known.[31] However, because the crystal structure of **1** has not been published previously and because we got new spectroscopic results (^{1}H NMR and $^{13}C\{^1H\}$ NMR data) for both of **1** and **2**, these data are also included in this paper. The crystal structure of **7** has also been published earlier,[35] but here we report two other unpublished polymorphic forms of this structure (**7a** in $P2_1/c$ and **7b** in $P\bar{1}$ space groups).

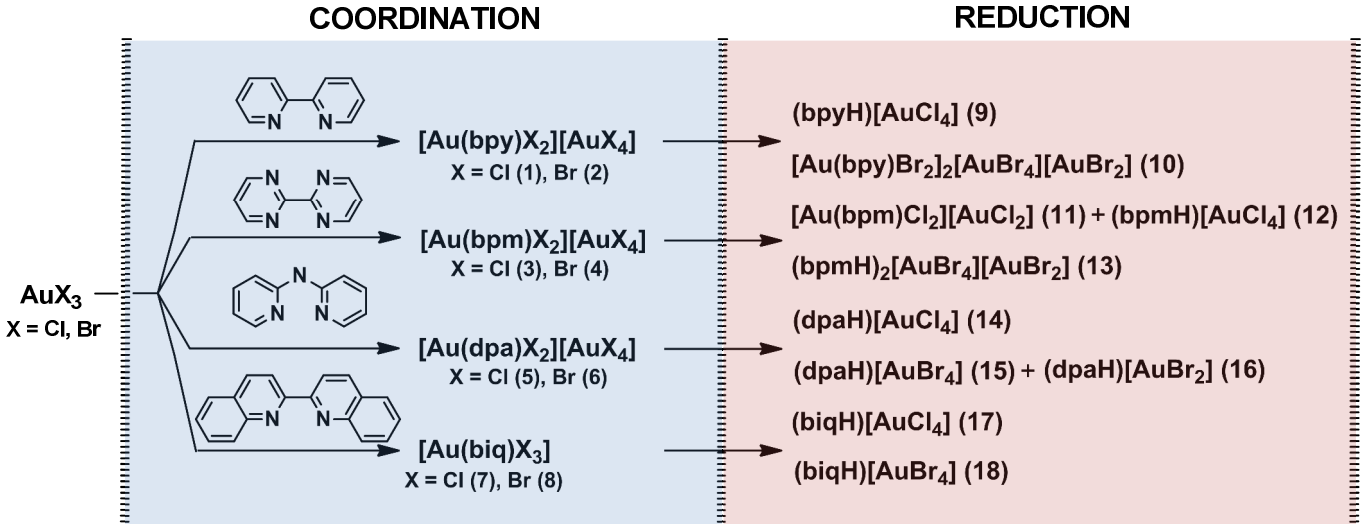

Scheme 2. Synthesis of complexes **1**–**8** (left) and their reduction by acetone providing **9**–**18** (right).

The choice of the starting materials was due to the fact that gold(III), being a hard metal center, readily reacts with nitrogen-containing ligands, and the chelate effect promotes the redistribution of halide ions to form tetrahaloaurate anions. The flat geometry and steric accessibility of the latter facilitate the formation of the aurophilic bonding in the formed double salts. The resulting compounds consist of singly charged ions, which are convenient since these compounds, in contrast to the di-ionic salts,[36] exhibit sufficiently high solubility in the most common organic solvents providing their easy recrystallization.

Reduction of compounds 1–8 by acetone

All complexes **1**–**8** were found to be prone to reduction of the metal centers by acetone, taken as the solvent, to gold(I) (**2**, **3**, **4**, and **6**) and to metallic gold (**1** and **3**–**8**). When the complexes were dissolved in acetone and left to stand in a closed flask at ambient temperature for several days (17 days for **1**, **2**, and **7**; 3 days for **3** and **4**; and 7 days for **5**, **6**, and **8**), formation of compounds **9**–**18** was observed (Scheme 2, right). Concurrently acetone was oxidized to chloroacetone or bromoacetone, and the formation of these species was confirmed by NMR. Similar reduction of gold(III) centers with bromide ligands by acetone were previously observed.[37,38] The reduction of **1**–**8** was

monitored by NMR and the structures of the reduction products **10**–**18** were confirmed by single-crystal X-ray diffraction.

Identification of aurophilic contacts

From the structural viewpoint it could be stated that aurophilic interaction occurs when the distance between gold centers is less than the sum of their van der Waals (vdW) radii. This simple criterion looks very convenient at the first glance. However, one should take into consideration that such radii cannot be unambiguously defined for metals and to date several sets of values of vdW radii based on different approaches have been suggested for the same atoms/ions,[38–47] varying the gold vdW radius from 1.66[40] to 2.43 Å.[42]

Nowadays the most widely used vdW radius for gold was proposed by Bondi,[40] that is the smallest one suggested. It is commonly accepted that a gold atom is involved in aurophilic bonding when the gold···gold distance is shorter than the sum of the Bondi's vdW radii (3.32 Å). However, it has also been argued that Bondi's vdW radii are too small by a systematic deviation[51] and too close to the corresponding covalent radii.[50] Therefore, the sum of Bondi's radii is not necessarily an indicative limit for aurophilic contacts and the length of the aurophilic bonds can exceed the sum of the Bondi's vdW radii. However, in such a case more detailed analysis of the gold-gold contact should be carried out. Other coexisting non-covalent interactions can also force gold atoms to be spatially close, and the effective vdW radius of gold should depend on the oxidation state,[52] which makes it even more difficult to recognize true aurophilic interactions simply by analyzing structural parameters of the system. Thus, in addition to structural analysis also detailed computational data is needed to confirm the aurophilicity.

In this work we used a combined approach to recognize aurophilicity based on structural analyses and computational results. The X-ray structures were studied computationally by using the topological charge density analysis based on Quantum Theory of Atoms in Molecules (QTAIM).[53] The main goal was to identify the existence of attractive intermolecular interactions between the gold centers in the solid state, and to establish their relative strength compared to the other typical weak interactions. Since single-crystal X-ray quality crystals were obtained for compounds **1**, **3**–**7**, and **10**–**18**, we only discuss these compounds. The crystallographic information of the structures is summarized in Table S1 and the selected bond lengths and angles are presented in Tables S2–S18 (see ESI†).

As the preliminary criterion of potential aurophilic contacts we used the sum of two Allinger's vdW radii of gold[42] (4.86 Å) insofar as to the best of our knowledge the Allinger's vdW radius is the largest among those reported in the literature.

Table 1. Gold···gold distances below sum of two Allinger's vdW radii of gold for **1**, **3**–**6**, and **10**–**16**.

Compound	Contact	Distance, Å	Symmetry codes
1	Au1···Au2^{i}	3.5250(1)	(i) *x*, 0.5–*y*, 0.5+*z*
	Au1···Au2^{ii}	4.1602(2)	(ii) *x*, 1.5–y, 0.5+z
3a	Au1···Au3^{iii}	3.6540(3)	(iii) –*x*, –0.5+*y*, 0.5–*z*
	Au1···Au2^{iv}	3.7904(3)	(iv) 1–*x*, –0.5+*y*, 0.5–*z*
	Au2···Au3^{v}	3.8701(3)	(v) *x*, *y*, *z*
3b	Au1···Au4^{vi}	4.7708(2)	(vi) –1+*x*, *y*, *z*
	Au3···Au4^{v}	4.0530(2)	
	Au3···Au3^{vii}	4.8294(2)	(vii) 2–*x*, 1–*y*, 2–*z*
4	Au1···Au2^{v}	3.5047(1)	
	Au1···Au2^{viii}	4.5327(2)	(viii) 1+*x*, *y*, *z*
5	Au1···Au2^{v}	3.7345(1)	
	Au1···Au1^{ix}	3.7467(1)	(ix) 1–*x*, 1–*y*, –*z*
6	Au1···Au2^{x}	4.3546(1)	(x) *x*, *y*, –1+*z*
10	Au1···Au2^{v}	4.3288(3)	
	Au1···Au3^{v}	4.5895(4)	
11	Au1···Au2^{xi}	3.6758(1)	(xi) 1–*x*, 1–*y*, *z*
	Au1···Au2^{xii}	4.5829(2)	(xii) 1–*x*, 1.5–*y*, 0.5+*z*
12	Au1···Au1^{xiii}	4.0358(2)	(xiii) –1–*x*, 2–*y*, –1–*z*
13	Au1···Au1^{xiv}	4.1382(1)	(xiv) 1–*x*, 1–*y*, 1–*z*
	Au2···Au2^{xv}	4.1992(1)	(xv) 1–*x*, –*y*, –*z*
14	Au1···Au1^{viii}	4.3301(1)	
15	Au1···Au1^{viii}	4.6997(4)	
16	Au1···Au1^{xvi}	4.8576(2)	(xv) 1–*x*, –*y*, 1–*z*

The aurophilic interactions confirmed by QTAIM are highlighted in green.

The gold···gold distances shorter than 4.86 Å were found in all structures apart from **7**, **17**, and **18** (Table 1). However, only in the structures of **1**, **3**–**5**, and **11** the gold atoms are positioned in such a way that a direct gold···gold contacts can be expected. Only in these structures the square planar gold moieties are arranged in face-to-face manner without significant Au···Au offset and tilting of the molecules. The QTAIM analysis of the structures of **1**, **3**–**5**, and **11** suggested the presence of the bond critical point (BCP) within the gold···gold contacts in all these cases (ρ(BCP) = 0.078–0.036 eÅ^{-3}) indicating their attractive nature. The energies of the Au^{III}···Au^{III} aurophilic bonds were found to be fairly low (9.3–3.6 kJmol^{-1}) in comparison with those predicted for Au^{III}···Au^{III} interactions (21–34 kJmol^{-1} at HF level of theory, 57 kJmol^{-1} at MP2 level of theory).[29] However, all in all the number of publications concerning the energetics of Au^{III}···Au^{III} interactions is quite limited preventing further analysis of the literature values.

Weak aurophilic contacts and other non-covalent interactions in the structures of 1–18

The QTAIM analysis revealed that **1**, **3**–**5**, and **11** exhibit weak aurophilic contacts. The strength of the aurophilic interactions was characterized in comparison with the other typical weak interactions determining the packing, and therefore these structures should be characterized in details.

The structure of compound **1** resembles closely both the known polymorph of **2**[31] and $[AuBr_2(bpy)][AuCl_4]$.[31] Likewise to the known analogues, **1** crystallizes in a face-to-face mode (Fig. 1) forming chain-like infinite sequence of alternating $[AuCl_2(bpy)]^+$ cations and $[AuCl_4]^-$anions.

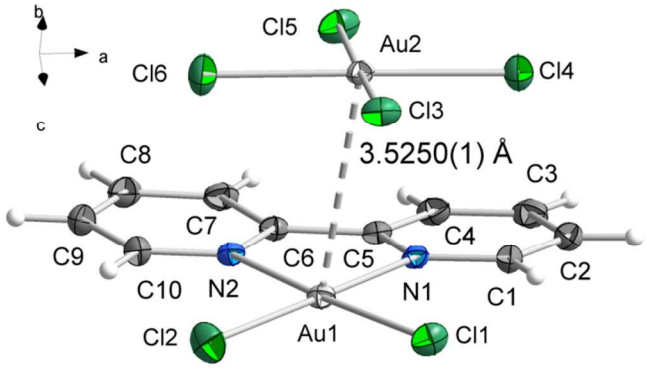

Fig. 1. Crystal structure of **1** with the atomic numbering scheme. The thermal ellipsoids are drawn at the 50% probability level.

The aurophilic interaction with E_{INT} = 8.9 kJmol^{-1} and ρ(BCP) = 0.074 eÅ^{-3} was observed within the ion pair between the gold centers of the cation and the anion, Au1 and Au2^{i}, respectively, which are located at a distance of 3.5250(1) Å (hereinafter the symmetry equivalent sites of the interacting gold atoms are defined in the Table 1). The absence of the aurophilic interaction between the gold centers of the cation and the anion of the adjacent ion pairs can be explained from two viewpoints. Firstly, the gold–gold distance between the ion pairs of 4.1602(2) Å is much higher in comparison with gold–gold distance within the ion pair (3.5250(1) Å). Secondly, in addition to the aurophilic interactions both Au1 and Au2^{i} centers participate in other weak interactions revealed by QTAIM. In particular, the Au1 center of the cation displays the Au1···Cl3 contact with the distance of 3.2249(1) Å, E_{INT} = 14.1 kJmol^{-1} and ρ(BCP) = 0.111 eÅ^{-3}, and Au2^{i} of the anion exhibits an interaction with the π system of bpy ligand. Thus, there is no room for the aurophilic interaction between the gold centers of the cation and the anion of the adjacent ion pairs. All these confirm our assumption on the importance of the molecular arrangement for the formation of weak aurophilic contacts. With regards to other weak interactions in the structure, both chlorines of the cation display the Cl–π interactions with the bpy ligand of the neighbouring cation and one of them has the halogen bond to a chlorine of the adjacent anion (Table S19 in ESI†). Cl atoms of the anion, in turn, in addition to the above-mentioned interactions, gives a number of Cl···H contacts (Table S19 in ESI†).

Complexes **3** and **4** featuring bpm ligand are also found to exhibit $Au^{III}\cdots Au^{III}$ contacts. Since the structure of bpm resembles closely the structure of bpy we expected that crystal structures of $[AuX_2(bpm)][AuX_4]$ (X = Cl **3**, X = Br **4**) should be similar to crystal structure of **1** and the known structure of **2**.[31] Indeed, structure of **4** is quite similar to those of **1** and **2**,[31] whereas **3** differs substantially from its bpy congeners. It crystallizes in two polymorphic forms, namely **3a** in *P*21/c and **3b** in *P*1 space groups, and instead of infinite sequence of alternating cations and anions, found in **1** and **2**, both **3a** and **3b** form the box-like supramolecular structures, which consist of two anions stacked in a face-to-face manner and surrounded by four cations, where each cation belongs to two adjacent boxes (Figs. 2 and 3). In **3a**, an aurophilic interaction was found between the Au1 and Au3^{iii} centers of the cation and the anion, but as the distance between Au1 and Au3^{iii} is somewhat longer than in the case of **1** (3.6540(3) and 3.5250(1) Å, respectively), also the interaction strength is weaker (E_{INT} = 6.5 kJmol^{-1} and ρ(BCP) = 0.059 eÅ^{-3}). Interestingly, the other cation–anion pair does not provide any aurophilic interactions between the two gold atoms, even if the Au1···Au2^{iv} distance is only slightly larger than for Au1···Au3^{iii}, 3.7904(3) vs. 3.6540(3) Å, respectively. Instead, there is a very weak attractive gold···gold interaction between two anionic units, even though the Au2···Au3^{v} distance is much larger (3.8701(3) Å), which indicates the weakness of the interaction (E_{INT} = 3.6 kJmol^{-1} and ρ(BCP) = 0.036 eÅ^{-3}). The reason for the absence of aurophilic bonding between Au1···Au2^{iv} is most probably the weak interaction of Au1 with Cl5 (Au1···Cl5 distance is 3.4033(2) Å, E_{INT} = 9.0 kJmol^{-1} and ρ(BCP) = 0.080 eÅ^{-3}). Such contact blocks the axial position of Au1 preventing the formation of aurophilic contact, which again demonstrates that the Au···Au distance is generally less important for the detection of aurophilicity than the molecular arrangement. Besides the aurophilic interactions and Au···Cl contacts, the boxes in **3a** are formed by the Cl–π interaction, halogen and hydrogen bonds (Table S20 in ESI†). The same interactions, but with π–π contacts instead of the aurophilicity, are found in the boxes of **3b** (Table S21 in ESI†). In both **3a** and **3b**, the sequence of boxes forms channels, which consist of the cations as walls and anions as fillings (Fig. 2, Fig. 3).

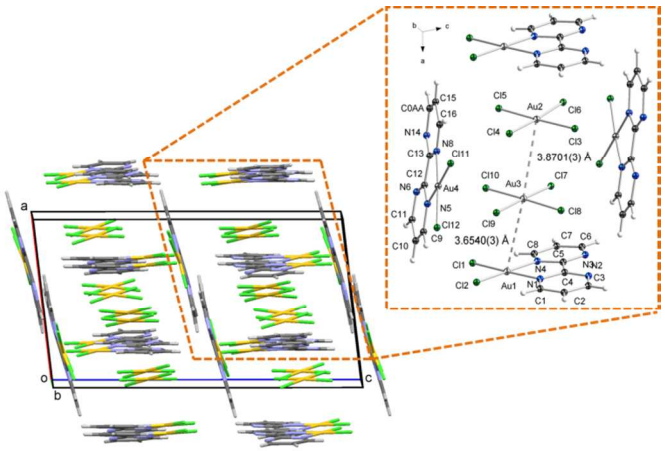

Fig. 2. Crystal structures of **3a** with the atomic numbering scheme and its supramolecular channel-like arrangement. The thermal ellipsoids are drawn at the 50% probability level.

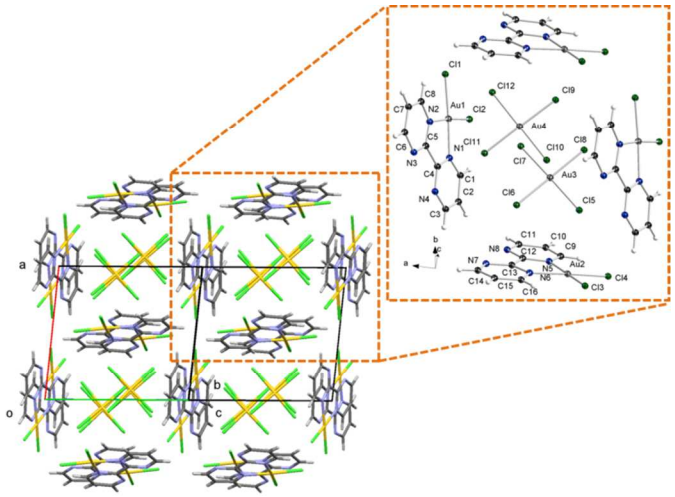

Fig. 3. Crystal structures of **3b** with the atomic numbering scheme and its supramolecular channel-like arrangement. The thermal ellipsoids are drawn at the 50% probability level.

Insofar as **3b**, which does not display any Au···Au bonding, crystallizes simultaneously with **3a**, which displays aurophilicity, we assume that the metallophilic bonding in **3a** is rather weak and is not capable to favor the formation of the certain polymorph.

Crystal structure of **4**, by contrast to **3a** and **3b**, consists of coplanar ion pairs, likewise in **1**, and in the known structures of **2**,[31] and $[AuBr_2(bpy)][AuCl_4]$[31] (Fig. 4) and the interactions in **4** are very similar to those observed in **1**.

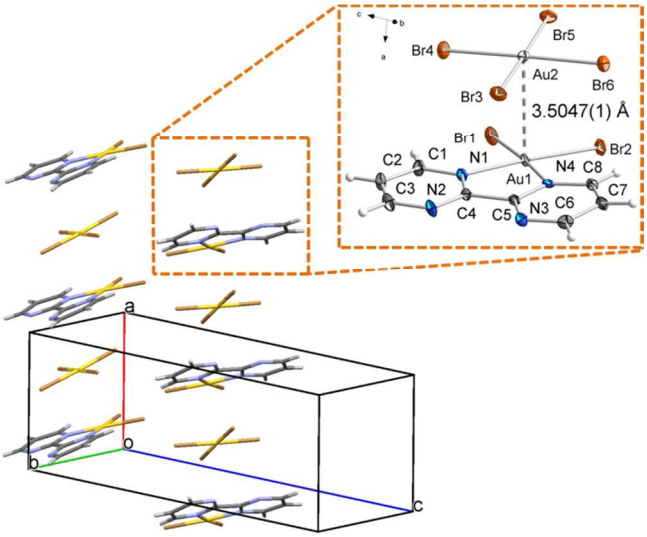

Fig. 4. Crystal structures of **4** with the atomic numbering scheme and its supramolecular stacked arrangement. The thermal ellipsoids are drawn at the 50% probability level.

In **4**, gold atoms of each cation are pseudo-octahedrally coordinated with the axial positions occupied by the gold and bromine atoms of the adjacent anions (the Au1···Au2^{v} distance is 3.5047(1) Å, E_{INT} = 9.3 kJmol^{-1}, and ρ(BCP) = 0.078 eÅ^{-3}; the Au1···Br5 distance is 3.2967(2) Å, E_{INT} = 14.7 kJmol^{-1} and ρ(BCP) = 0.117 eÅ^{-3}). The aurophilic contact was detected only within the ion pair, the gold atoms of the neighboring ion pairs do not display such contacts as in the case of **1**. Noteworthy that in **4** the aurophilic contact is the shortest and the strongest among such contacts in studied **1**, **3a**, **4**, **5**, and **11** species. The gold atom of the anion, in addition to the aurophilic interaction, displays also the contact with the π system of the bpm ligand. In addition to the aurophilicity, the Au···Br and Au–π contacts, the structure of **4** exhibit the Br–π contacts and both halogen and hydrogen bonds (Table S22 in ESI†).

The aforementioned interactions provide the infinite stacks of alternating ions (Fig. 4). Such a significant distinction between the channel-like supramolecular structures of **3a** and **3b**, on the one hand, and stacked supramolecular structure of **4**, on the other hand, can be explained in terms of steric hindrance and difference in strength of halogen bonds and halogen–π contacts involving the Cl (in **3a** and **3b**) and Br atoms (in **4**), which should be generally higher in the latter case.[54]

Double salt **5** also exhibits weak metallophilic contacts. As it was observed in the corresponding X-ray study, its unit cell contains the acetonitrile of crystallization and two halves of crystallographically independent anions (Fig. 5).

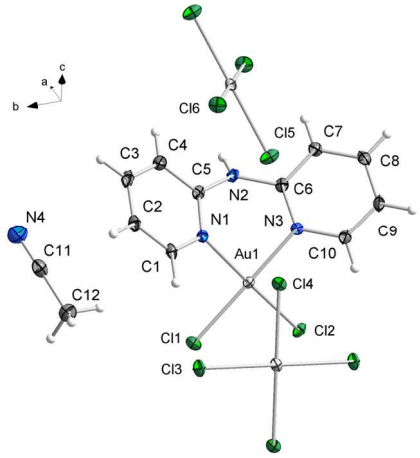

Fig. 5. Crystal structure of **5** with the atomic numbering scheme. The thermal ellipsoids are drawn at the 50% probability level.

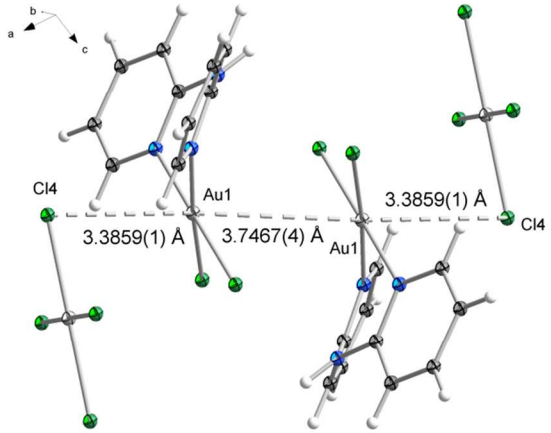

Fig. 6. The sequence of the main weak interactions in **5**. The thermal ellipsoids are drawn at the 50% probability level.

In the structure of **5**, the only observed aurophilic interaction is between two cationic building blocks with the Au1···Au1^{ix} distance of 3.7467(1) Å, E_{INT} = 5.8 kJmol^{-1} and ρ(BCP) = 0.053 eÅ^{-3}. The gold atoms of each cation also interact with the Cl ligand of the adjacent anion thus forming a pseudo-octahedral coordination sphere around the gold atom. According to the QTAIM calculations, the Au···Cl interaction is stronger than the aurophilic one (the Au1···Cl4 distance is 3.3859(1) Å, E_{INT} = 9.6 kJmol^{-1}, and ρ(BCP) = 0.083 eÅ^{-3}) and located at the same axis than the Au···Au interactions (Fig. 6). Despite the distance between the gold atoms of the cation and the anion is slightly shorter than that between two cations (3.7345(1) vs. 3.7467(1) Å), the aurophilic interaction between the anions and the cations was not observed by QTAIM calculations. The reason for this most probably lies within the non-planarity of the bulky dpa ligand, which directs the anions in a relatively tilted position and enables the formation of the pseudo-octahedral symmetry via using the Cl ligands only. In **5**, the aurophilic interactions are most probably formed as a results of the more important Au···Cl, Cl···Cl, Cl–π contacts and hydrogen bonds (Table S23 in ESI†).

Among **9**–**18**, derived from the reduction with acetone (see above), only **11** displays a metallophilic bonding. The compound crystallizes as a mixed-valence system with the Au^{III} center of the cation and the Au^{I} center of the anion. Each Au^{I} is aurophilically connected to Au^{III} of the cation from one side (the Au1···Au2 distance is 3.6758(2) Å, E_{INT} = 7.0 kJmol^{-1}, and ρ(BCP) = 0.065 eÅ^{-3}), and from another one it displays an Au–π interaction (Fig. 7). The Au1···Au2 interaction is further supported by the additional Au1···Cl3 interaction (the Au1···Cl3 distance is 3.4954(9) Å), with strength very similar to the aurophilic bonding (E_{INT} = 7.8 kJmol^{-1} and ρ(BCP) = 0.071 eÅ^{-3}). The structure of **11** possesses also halogen and hydrogen bonds and Cl–π contacts (Table S24 in ESI†).

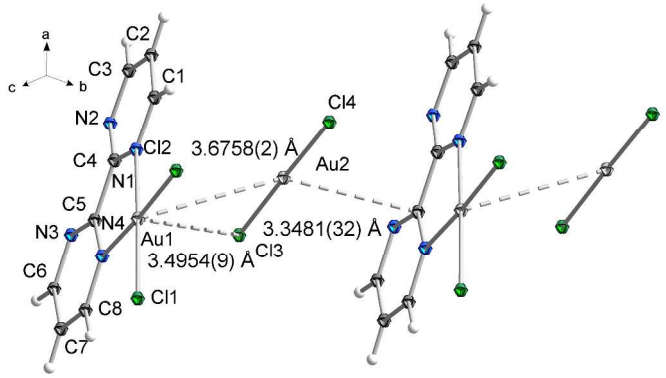

Fig. 7. Crystal structure of **11** with the atomic numbering scheme. Main weak interactions are shown with dashed line. The thermal ellipsoids are drawn at the 50% probability level.

Experimental

Materials and methods

Ligands, solvents, and gold salts used in the syntheses were obtained from commercial sources (Aldrich, Merck, Alfa Aesar) and used as received. Elemental analyses for carbon, hydrogen, and nitrogen was carried out with Elenentar Vario Micro instrument. The ^{1}H and ^{13}C{^{1}H} NMR spectra were measured on a Bruker-DPX300 instrument at ambient temperature. Yields are based on gold.

X-ray structure determination

All crystals were obtained by a slow evaporation of corresponding solutions at 4 °C. Crystals were immersed in cryo-oil, mounted in a MiTeGen loop, and measured at a temperature of 120 K (**1**, **3a**, **3b**, **4**, **5**, **7b**, and **10**–**18**) or 150 K (**7a**). The X-ray diffraction data were collected on a Nonius KappaCCD, Bruker Axs KappaApexII, or Agilent SuperNova diffractometers using Mo Kα radiation (λ = 0.71073 Å). The Apex2,[55] Saint,[56] and Denzo/Scalepack[57] program packages were used for cell refinements and data reductions. The structures were solved by direct methods using Shelxs 97[58] or

SUPERFLIP[59] program with the Olex 2[60] graphical user interface. A semi-empirical or numerical absorption correction (SADABS[61] or Xprep in Shelxtl[62]) was applied to all data. Structural refinements were carried out using SHELXL-97 or SHELXL-2014.[58]

In all the structures except **17** and **18**, hydrogen atoms were positioned geometrically and constrained to ride on their parent atoms, with C–H 0.95 Å, N–H = 0.88 Å, and U_{iso} = 1.2 U_{eq} (parent atom). In the structures of **17** and **18**, the NH hydrogen atoms were located from the difference Fourier map but constrained to ride on their parent nitrogen with U_{iso} = 1.2 U_{eq}. Other hydrogen atoms were positioned geometrically and constrained to ride on their parent atoms, with C–H 0.95 Å and U_{iso} = 1.2 U_{eq} (parent atom).

In the structure of **7a**, both Au atoms were disordered over two sites (Au1/Au1C and Au1B/Au1D) with occupancy ratio 0.06/0.94 and 0.21/0.79. The disordered gold atoms were restrained to have the same U_{ij} components. In the structure of **12**, the NH hydrogen was disordered over two sites (on N5 and N6) with equal occupancy ratio. In the structures of **14**, **15**, and **16**, the bridging amine nitrogens were disordered over two alternative sites around the centers of symmetry with equal occupancies. Due to this disorder also the pyridine nitrogens (N2) and its neighboring carbons (C1) were disordered over alternative positions with equal occupancies. Only one of the pyridine nitrogen was protonated in all three compounds.

The crystal structures of **1**, **3**, **4**, **5**, and **11**, which possess the aurophilic bonding, are presented in Figs. 1–5 and 7, respectively. The crystal structures of the rest compounds (**6**, **7a**, **7b**, **10**, and **12**–**18**) are given in Figs. S1–S11, respectively. The crystallographic details are given in Table S1 in ESI†.

Computational details

All models were calculated with the Gaussian09 program package[63] at the DFT level of theory with a hybrid density functional PBE0.[64] The basis set consisted of a quasi-relativistic effective core potential basis set def2-TZVPPD[65] for metal atoms, the standard all-electron basis sets 6-311+G(d) for N, Cl, and Br atoms and 6-31G(d,p) for C and H atoms.

To obtain the electronic properties of the complexes, we performed topological charge density analysis with the QTAIM method,[53] which allowed the access to the nature of the bonding via calculating different properties of the electron density at the bond critical points (BCPs). The analysis was done with the AIMALL program[66] using the wavefunctions obtained from the DFT calculations with the models cut directly from the experimental crystal structures. For all structures, the models included two cation-anion pairs, resulting in a neutral total charge of the system.

Synthetic work

Synthesis of the complexes 1–8. Gold(III) halide (100 mg, 0.33 mmol of $AuCl_3$, 100 mg, 0.23 mmol of $AuBr_3$) and the appropriate amount of bpy (26 mg, 0.17 mmol in the case of $AuCl_3$, 18 mg, 0.12 mmol in the case of $AuBr_3$), bpm (26 mg, 0.16 mmol in the case of $AuCl_3$, 18 mg, 0.11 mmol in the case of $AuBr_3$), dpa (28 mg, 0.16 mmol in the case of $AuCl_3$, 20 mg, 0.12 mmol in the case of $AuBr_3$), or biq (42 mg, 0.16 mmol in the case of $AuCl_3$, 29 mg, 0.11 mmol in the case of $AuBr_3$) were dissolved in C_2H_5CN (5 mL) and the solutions were mixed. The reaction mixtures were left to stand at an ambient temperature for 12 h. The resulting yellow (for **1**, **3**, and **7**) or red (for **2**, **4**–**6**, and **8**) solutions with the precipitates of the similar colour were evaporated under vacuum to the volume of 0.5 ml each and cooled down to 4 °C. The obtained solid residues were filtered off, washed with cold acetonitrile (1 ml) and diethyl ether (2 ml) and dried under vacuum. The isolated yields are 119 mg, 94% of **1**, 100 mg, 85% of **2**, 112 mg, 89% of **3**, 110 mg, 93% of **4**, 120 mg, 94 % of **5**, 104 mg, 87% of **6**, 128 mg, 90% of **7**, and 107 mg, 83% of **8**. Crystals of **1** and **3**–**7** suitable for single-crystal X-ray diffraction were obtained by the recrystallization of the corresponding materials from acetonitrile at 4 °C.

Reduction of 1–8 with formation of 9–18. Each of **1**–**8** (100 mg, 0.13 mmol of **1**, 100 mg, 0.10 mmol of **2**, 100 mg, 0.13 mmol of **3**, 100 mg, 0.10 mmol of **4**, 100 mg, 0.13 mmol of **5**, 100 mg, 0.10 mmol of **6**, 100 mg, 0.18 mmol of **7**, and 100 mg, 0.14 mmol of **8**) was dissolved in acetone (10 ml) and left to stand at the ambient temperature in the closed flask for 17 days (**1**, **2**, and **7**), 3 days (**3** and **4**), or 7 days (**5**, **6**, and **8**). The resulting solutions were filtered and subjected the ^{1}H NMR analysis to confirm the presence of chloroacetone or bromoacetone. Subsequently the solutions were evaporated under vacuum to the volume of 0.5 ml each and cooled down to 4 °C. The obtained yellow (in the cases of **9**, **11**, **12**, and **17**), red (in the cases of **10** and **16**), brown (in the cases of **13**, **15**, and **18**), or orange (in the case of **14**) solid residues were filtered off, washed with cold acetone (1 ml) and diethyl ether (2 ml) and dried under vacuum furnishing the compounds **9**–**18**. The yields are 50 mg, 39% of **9**, 69 mg, 72% of **10**, 47 mg, 52% of **11**, 25 mg, 16% of **12**, 46 mg, 39% of **13**, 57 mg, 43 % of **14**, 32 mg, 23% of **15**, 16 mg, 15% of **16**, 47 mg, 43% of **17**, 31 mg, 34% of **18**. The reduction was also monitored by ^{1}H and ^{13}C{^{1}H} NMR experiments. Compounds **1**–**8** were dissolved in deuteroacetone and left to stand at an ambient temperature in the NMR tubes. The daily measured ^{1}H and ^{13}C{^{1}H} NMR spectra displayed the gradual disappearance of the signals of initial compounds **1**–**8** and emergence of the signals of reduction products **9**–**18**.

[$AuCl_2$(bpy)][$AuCl_4$] (**1**). ^{1}H NMR spectrum ($(CD_3)_2CO$), δ): 9.65 (d, 6.1 Hz, 2H, HC(6), hereinafter the atomic position numbering is given according to IUPAC nomenclature), 9.05 (d, 6.1 Hz, 2H, HC(3)), 8.88 (t, 6.1 Hz, 2H, HC(4)), 8.33 (t, 6.1 Hz, 2H, HC(5)). ^{13}C{^{1}H} spectrum ($(CD_3)_2CO$), δ): 157.2 (C(2)), 148.7 (C(6)), 147.0 (C(4)), 130.9 (C(5)), 127.8 (C(3)).

[$AuBr_2$(bpy)][$AuBr_4$] (**2**). ^{1}H NMR spectrum ($(CD_3)_2CO$), δ): 9.89 (d, 6.7 Hz, 2H, HC(6)), 9.04 (d, 6.7 Hz, 2H, HC(3)), 8.86 (t, 6.7 Hz, 2H, HC(4)), 8.31 (t, 6.7 Hz, 2H, HC(5)). ^{13}C{^{1}H} spectrum ($(CD_3)_2CO$), δ): 157.4 (C(2)), 149.6 (C(6)), 146.4 (C(4)), 130.1 (C(5)), 127.6 (C(3)).

[$AuCl_2$(bpm)][$AuCl_4$] (**3**). Found: C, 12.48; H, 0.85; N, 7.40 (Calcd. for $C_8H_6N_4Cl_6Au_2$: C, 12.56; H, 0.79; N, 7.33). ^{1}H

NMR spectrum ($(CD_3)_2CO$), δ): 9.99 (d, 5.6 Hz, 2H), 9.77 (d, 5.6 Hz, 2H) (HC(6) and HC(4)), 8.53 (t, 5.6 Hz, 2H, HC(5)). $^{13}C\{^1H\}$ NMR spectrum ($(CD_3)_2CO$), δ): 166.0 C(2)), 160.1, 155.5 (HC(6) and HC(4)), 128.2 (HC(5)).

[AuBr$_2$(bpm)][AuBr$_4$] (**4**). Found: C, 9.15; H, 0.69; N, 5.30 (Calcd. for $C_8H_6N_4Br_6Au_2$: C, 9.31; H, 0.59; N, 5.43). ^1H NMR spectrum ($(CD_3)_2CO$), δ): 10.18 (d, 5.4 Hz, 2H), 9.78 (d, 5.4 Hz, 2H) (HC(6) and HC(4)), 8.51 (t, 5.4 Hz, 2H, HC(5)). $^{13}C\{^1H\}$ NMR spectrum ($(CD_3)_2CO$), δ): 167.1 C(2)), 160.7, 155.9 (HC(6) and HC(4)), 127.3 (HC(5)).

[AuCl$_2$(dpa)][AuCl$_4$] (**5**). Found: C, 15.57; H, 1.22; N, 5.31 (Calcd. for $C_{10}H_9N_3Cl_6Au_2$: C, 15.44; H, 1.16; N, 5.40). ^1H NMR spectrum ($(CD_3)_2CO$), δ): 11.34 (s, br, 1H, NH_{amine}), 8.95 (d, 7.0 Hz, 2H, HC(6)), 8.41 (t, 7.0 Hz, 2H, HC(4)), 7.86 (d, 7.0 Hz, 2H, HC(3)), 7.69 (t, 7.0 Hz, 2H, HC(5)). $^{13}C\{^1H\}$ NMR spectrum ($(CD_3)_2CO$), δ): 148.3 (C(2)), 147.9 (C(6)), 146.2 (C(4)), 122.5 (C(5)), 118.3 (C(3)).

[AuBr$_2$(dpa)][AuBr$_4$] (**6**). Found: C, 11.41; H, 0.75; N, 4.20 (Calcd. for $C_{10}H_9N_3Br_6Au_2$: C, 11.50; H, 0.87; N, 4.02). ^1H NMR spectrum ($(CD_3)_2CO$), δ): 11.20 (s, br, 1H, NH_{amine}), 9.10 (d, 7.3 Hz, 2H, HC(6)), 8.40 (t, 7.3 Hz, 2H, HC(4)), 7.85 (d, 7.3 Hz, 2H, HC(3)), 7.65 (t, 7.3 Hz, 2H, HC(5)). $^{13}C\{^1H\}$ NMR spectrum ($(CD_3)_2CO$), δ): 149.5 (C(2)), 148.3 (C(6)), 146.8 (C(4)), 122.0 (C(5)), 117.7 (C(3)).

[AuCl$_3$(biq)] (**7**). Found: C, 38.56; H, 2.10; N, 4.89 (Calcd. for $C_{18}H_{12}Cl_3N_2Au$: C, 38.63; H, 2.16; N, 5.01). ^1H NMR spectrum ($(CD_3)_2CO$), δ): 9.14 (d, 8.7 Hz, 2H, HC(3)), 9.02 (d, 8.7 Hz, 2H, HC(4)), 8.84 (d, 7.9 Hz, 2H, HC(8)), 8.31 (d, 7.9 Hz, 2H, HC(5)), 8.20 (t, 7.9 Hz, 2H, HC(7)), 7.96 (t, 7.9 Hz, 2H, HC(6)). $^{13}C\{^1H\}$ NMR spectrum ($(CD_3)_2CO$), δ): 153.3 (C(2)), 146.8 (C(8a)), 142.7 (C(4)), 133.8 (C(8)), 130.9 (C(7)), 130.6 (C(4a)), 130.0 (C(5)), 129.6 (C(6)), 123.7 (C(3)).

[AuBr$_3$(biq)] (**8**). Found: C, 31.20; H, 1.75; N, 4.04 (Calcd. for $C_{18}H_{12}Br_3N_2Au$: C, 31.35; H, 1.93; N, 3.89). ^1H NMR spectrum ($(CD_3)_2CO$), δ): 9.09 (d, 8.8 Hz, 2H, HC(3)), 9.00 (d, 8.8 Hz, 2H, HC(4)), 8.83 (d, 8.0 Hz, 2H, HC(8)), 8.30 (d, 8.0 Hz, 2H, HC(5)), 8.17 (t, 8.0 Hz, 2H, HC(7)), 7.95 (t, 8.0 Hz, 2H, HC(6)). $^{13}C\{^1H\}$ NMR spectrum ($(CD_3)_2CO$), δ): 152.2 (C(2)), 147.1 (C(8a)), 142.5 (C(4)), 133.5 (C(8)), 130.5 (C(7)), 130.4 (C(4a)), 129.9 (C(5)), 129.5 (C(6)), 123.7 (C(3)).

(bpyH)[AuCl$_4$] (**9**). Found: C, 24.07; H, 1.76; N, 5.45 (Calcd. for $C_{10}H_9N_2Cl_4Au$: C, 24.22; H, 1.83; N, 5.65). ^1H NMR spectrum ($(CD_3)_2CO$), δ): 9.13 (d, 7.4 Hz, 2H, HC(6)), 8.84 (d, 7.4 Hz, 2H, HC(3)), 8.67 (t, 7.4 Hz, 2H, HC(4)), 8.12 (t, 7.4 Hz, 2H, HC(5)). $^{13}C\{^1H\}$ spectrum ($(CD_3)_2CO$), δ): 154.2 (C(2)), 147.4 (C(6)), 144.8 (C(4)), 128.7 (C(5)), 124.6 (C(3)).

[AuBr$_2$(bpy)]$_2$[AuBr$_4$][AuBr$_2$] (**10**). Found: C, 12.86; H, 1.09; N, 2.63 (Calcd. for $C_{20}H_{16}N_4Br_{10}Au_4$: C, 12.65; H, 0.85; N, 2.95). ^1H NMR spectrum ($(CD_3)_2CO$), δ): 9.85 (d, 6.4 Hz, 2H, HC(6)), 9.00 (d, 6.4 Hz, 2H, HC(3)), 8.89 (t, 6.4 Hz, 2H, HC(4)), 8.32 (t, 6.4 Hz, 2H, HC(5)). $^{13}C\{^1H\}$ spectrum ($(CD_3)_2CO$), δ): 157.2 (C(2)), 149.9 (C(6)), 146.3 (C(4)), 130.1 (C(5)), 127.6 (C(3)).

[AuCl$_2$(bpm)][AuCl$_2$] (**11**). Found: C, 13.76; H, 0.98; N, 8.00 (Calcd. for $C_8H_6N_4Cl_4Au_2$: C, 13.85; H, 0.87; N, 8.07). ^1H NMR spectrum ($(CD_3)_2CO$), δ): 9.93 (d, 5.5 Hz, 2H), 9.78 (d, 5.5 Hz, 2H) (HC(6) and HC(4)), 8.49 (t, 5.5 Hz, 2H, HC(5)). $^{13}C\{^1H\}$ NMR spectrum ($(CD_3)_2CO$), δ): 166.4 C(2)), 159.8, 155.1 (HC(6) and HC(4)), 128.3 (HC(5)).

(bpmH)[AuCl$_4$] (**12**). Found: C, 19.44; H, 1.70; N, 11.46 (Calcd. for $C_8H_7N_4Cl_4Au$: C, 19.30; H, 1.42; N, 11.25). ^1H NMR spectrum ($(CD_3)_2CO$), δ): 9.53 (d, 5.2 Hz, 4H, HC(4) and HC(6)), 8.27 (t, 5.2 Hz, 2H, HC(5)). $^{13}C\{^1H\}$ NMR spectrum ($(CD_3)_2CO$), δ): 159.9 (C(2)), 156.2 (C(3) and C(5)), 125.4 (C(4)).

(bpmH)$_2$[AuBr$_4$][AuBr$_2$] (**13**). Found: C, 16.05; H, 1.24; N, 9.35 (Calcd. for $C_{16}H_{14}N_8Br_6Au_2$: C, 16.13; H, 1.18; N, 9.40). ^1H NMR spectrum ($(CD_3)_2CO$), δ): 9.61 (d, 5.7 Hz, 4H, HC(4) and HC(6)), 8.33 (t, 5.7 Hz, 2H, HC(5)). $^{13}C\{^1H\}$ NMR spectrum ($(CD_3)_2CO$), δ): 159.9 (C(2)), 156.3 (C(3) and C(5)), 125.4 (C(4)).

(dpaH)[AuCl$_4$] (**14**). Found: C, 23.43; H, 2.20; N, 8.03 (Calcd. for $C_{10}H_{10}N_3Cl_4Au$: C, 23.51; H, 1.97; N, 8.22). ^1H NMR spectrum ($(CD_3)_2CO$), δ): 8.49 (d, 7.9 Hz, 2H, HC(6)), 8.20 (t, 7.9 Hz, 2H, HC(4)), 7.45 (d, 7.9 Hz, 2H, HC(3)), 7.40 (t, 7.9 Hz, 2H, HC(5)). $^{13}C\{^1H\}$ NMR spectrum ($(CD_3)_2CO$), δ): 147.8 (C(2)), 143.6 (C(6)), 142.0 (C(4)), 119.3 (C(5)), 115.4 (C(3)).

(dpaH)[AuBr$_4$] (**15**). Found: C, 17.40; H, 1.52; N, 6.00 (Calcd. for $C_{10}H_{10}N_3Br_4Au$: C, 17.43; H, 1.46; N, 6.10). ^1H NMR spectrum ($(CD_3)_2CO$), δ): 11.71 (s, br, 1H, NH_{amine}), 8.47 (d, 5.5 Hz, 2H, HC(6)), 8.17 (t, 5.5 Hz, 2H, HC(4)), 7.63 (d, 5.5 Hz, 2H, HC(3)), 7.37 (t, 5.5 Hz, 2H, HC(5)). $^{13}C\{^1H\}$ NMR spectrum ($(CD_3)_2CO$), δ): 152.6 (C(2)), 143.6 (C(6)), 142.0 (C(4)), 119.3 (C(5)), 115.4 (C(3)).

(dpaH)[AuBr$_2$] (**16**). Found: C, 22.60; H, 1.78; N, 7.72 (Calcd. for $C_{10}H_{10}N_3Br_2Au$: C, 22.71; H, 1.91; N, 7.94). ^1H NMR spectrum ($(CD_3)_2CO$), δ): 8.49 (d, 6.6 Hz, 2H, HC(6)), 8.20 (t, 6.6 Hz, 2H, HC(4)), 7.50 (d, 6.6 Hz, 2H, HC(3)), 7.39 (t, 6.6 Hz, 2H, HC(5)). $^{13}C\{^1H\}$ NMR spectrum ($(CD_3)_2CO$), δ): 150.2 (C(2)), 143.4 (C(6)), 142.0 (C(4)), 119.3 (C(5)), 115.4 (C(3)).

(biqH)[AuCl$_4$] (**17**). Found: C, 36.48; H, 2.34; N, 4.45 (Calcd. for $C_{18}H_{13}N_2Cl_4Au$: C, 36.27; H, 2.20; N, 4.70). ^1H NMR spectrum ($(CD_3)_2CO$), δ): 9.14 (d, 8.7 Hz, 2H, HC(3)), 9.01 (d, 8.7 Hz, 2H, HC(4)), 8.83 (d, 8.3 Hz, 2H, HC(8)), 8.32 (d, 8.3 Hz, 2H, HC(5)), 8.20 (t, 8.3 Hz, 2H, HC(7)), 7.96 (t, 8.3 Hz, 2H, HC(6)). $^{13}C\{^1H\}$ NMR spectrum ($(CD_3)_2CO$), δ): 153.3 (C(2)), 146.8 (C(8a)), 142.7 (C(4)), 133.8 (C(8)), 130.9 (C(7)), 130.6 (C(4a)), 130.0 (C(5)), 129.6 (C(6)), 123.7 (C(3)).

(biqH)[AuBr$_4$] (**18**). Found: C, 27.80; H, 1.85; N, 3.46 (Calcd. for $C_{18}H_{13}N_2Br_4Au$: C, 27.94; H, 1.69; N, 3.62). ^1H NMR spectrum ($(CD_3)_2CO$), δ): 9.14 (d, 8.6 Hz, 2H, HC(3)), 9.01 (d, 8.6 Hz, 2H, HC(4)), 8.49 (d, 8.5 Hz, 2H, HC(8)), 8.35 (d, 8.5 Hz, 2H, HC(5)), 8.15 (t, 8.5 Hz, 2H, HC(7)), 7.96 (t, 8.5 Hz, 2H, HC(6)). $^{13}C\{^1H\}$ NMR spectrum ($(CD_3)_2CO$), δ): 157.2 (C(2)), 145.2 (C(8a)), 143.8 (C(4)), 135.1 (C(8)), 131.1 (C(7)), 130.5 (C(4a)), 129.9 (C(5)), 129.7 (C(6)), 126.1 (C(3)).

Conclusions

We have synthesized a series of new gold(III) double salts exhibiting the close $Au^{III}\cdots Au^{III}$ contacts. Weak aurophilic nature of these contacts was confirmed by computational

QTAIM analysis. We have demonstrated that the gold···gold distance should not be considered as the ultimate factor for the detection of aurophilicity, at least at the weakest limit of the interaction strength. Instead, one should consider also the packing of the compound, paying attention to the orientation of the units and the weak interactions other than aurophilicity.

Acknowledgements

Financial support provided by the Academy of Finland (project 139571 MH and ANC) is gratefully acknowledged. ANC and VYK are also indebted to RFBR and Saint Petersburg State University for grants 13-03-12411-ofim and 12.38.225.2014, respectively.

Notes and references

[a] Department of Chemistry, University of Jyväskylä, P.O. Box 35, FI-40014 Jyväskylä, Finland
[b] Institute of Chemistry, Saint Petersburg State University, 198504 Stary Petergof, Russian Federation
[c] Department of Chemistry, University of Eastern Finland, P.O.Box 111, FI-80101 Joensuu, Finland

† Electronic Supplementary Information (ESI) available: Crystallographic data for **1**, **3a**, **3b**, **4**, **5**, **6**, **7a**, **7b**, and **10–18 (**CCDC 1029113, 1029123–1029126, 1407541, 1029127, 1029128, 1029114–1029122, respectively**)**, tables of selected bond lengths and angles for **1**, **3a**, **3b**, **4**, **5**, **6**, **7a**, **7b**, and **10–18**, tables of weak interactions for **1**, **3a**, **3b**, **4**, **5**, and **11**, and thermal ellipsoid plots for **7a**, **7b**, and **10–18** are given in the supporting information. See DOI: 10.1039/b000000x/

1. J. C. Vickery, M. M. Olmstead, E. Y. Fung, and A. L. Balch, *Angew. Chemie, Int. Ed. Eng.*, 1997, **36**, 1179–1181.
2. V. W. Yam and K. K. Lo, *Chem. Soc. Rev.*, 1999, **28**, 323–334.
3. C.-M. Che, M.-C. Tse, M. C. W. Chan, K.-K. Cheung, D. L. Phillips, and K.-H. Leung, *J. Am. Chem. Soc.*, 2000, **122**, 2464–2468.
4. A. F. Heyduk, D. J. Krodel, E. E. Meyer, and D. G. Nocera, *Inorg. Chem.*, 2002, **41**, 634–636.
5. M. Stender, R. L. White-morris, M. M. Olmstead, and A. L. Balch, *Inorg. Chem.*, 2003, **42**, 4504–4506.
6. A. L. Balch, *Gold Bull.*, 2004, **37**, 45–50.
7. N. L. Coker, J. A. . Krause Bauer, and R. C. Elder, *J. Am. Chem. Soc.*, 2004, **126**, 12–13.
8. X. Liu, G. Guo, M. Fu, X. Liu, M. Wang, and J. Huang, *Inorg. Chem.*, 2006, **45**, 3679–3685.
9. E. J. Fernández, A. Laguna, and J. M. López-de-Luzuriaga, *Dalton. Trans.*, 2007, 1969–1981.
10. B. Liu, W. Chen, and S. Jin, *Organometallics*, 2007, **26**, 3660–3667.
11. D. B. Leznoff, B.-Y. Xue, C. L. Stevens, A. Storr, R. C. Thompson, and B. O. Patrick, *Polyhedron*, 2001, **20**, 1247–1254.
12. S. M. Drew, L. I. Smith, K. A. McGee, and K. R. Mann, *Chem. Mater.*, 2009, **21**, 3117–3124.
13. M. J. Katz, T. Ramnial, H.-Z. Yu, and D. B. Leznoff, *J. Am. Chem. Soc.*, 2008, **130**, 10662–10673.
14. E. Laurila, R. Tatikonda, L. Oresmaa, P. Hirva, and M. Haukka, *CrystEngComm*, 2012, **14**, 8401.
15. E. Laurila, L. Oresmaa, M. Niskanen, P. Hirva, and M. Haukka, *Cryst. Growth Des.*, 2010, **10**, 3775–3786.
16. V. W.-W. Yam, K. M.-C. Wong, and N. Zhu, *J. Am. Chem. Soc.*, 2002, **124**, 6506–6507.
17. M. Mitsumi, H. Goto, S. Umebayashi, Y. Ozawa, M. Kobayashi, T. Yokoyama, H. Tanaka, S. Kuroda, and K. Toriumi, *Angew. Chem. Int. Ed.*, 2005, **44**, 4164–4168.
18. A. Guijarro, O. Castillo, A. Calzolari, P. J. S. Miguel, C. J. Go, and R. Felice, *Inorg. Chem.*, 2008, **47**, 9736–9738.
19. M. Mitsumi, H. Ueda, K. Furukawa, Y. Ozawa, K. Toriumi, and M. Kurmoo, *J. Am. Chem. Soc.*, 2008, **130**, 14102–14104.
20. S. Myllynen and M. Wasberg, *Electrochem. commun.*, 2009, **11**, 1453–1456.
21. H. Schmidbaur, *Gold Bull.*, 1990, **23**, 11–21.
22. P. Pyykkö, *Angew. Chem. Int. Ed.*, 2004, **43**, 4412–4456.
23. H. Schmidbaur and A. Schier, *Chem. Soc. Rev.*, 2008, **37**, 1931–1951.
24. P. Pyykkö, *Chem. Rev.*, 1997, **97**, 597–636.
25. P. Schwerdtfeger, *Heteroat. Chem.*, 2002, **13**, 578–584.
26. P. Pyykkö, *Inorg. Chim. Acta*, 2005, **358**, 4113–4130.
27. P. Pyykkö, *Chem. Soc. Rev.*, 2008, **37**, 1967–1997.
28. F. Mendizabal, G. Zapata-Torres, and C. Olea-Azar, *Chem. Phys. Lett.*, 2003, **382**, 92–99.
29. F. Mendizabal and P. Pyykkö, *Phys. Chem. Chem. Phys.*, 2004, **6**, 900–905.
30. T. M. Klapoetke, B. Krumm, J.-C. Galvez-Ruiz, and H. Noeth, *Inorg. Chem.*, 2005, **44**, 9625–9627.
31. R. Hayoun, D. K. Zhong, A. L. Rheingold, and L. H. Doerrer, *Inorg. Chem.*, 2006, **45**, 6120–6122.
32. H. Schmidbaur and A. Schier, *Chem. Soc. Rev.*, 2012, **41**, 370–412.

33. J. S. Ovens, K. N. Truong, and D. B. Leznoff, *Dalton. Trans.*, 2012, **41**, 1345–1351.

34. L. H. Doerrer, *Comments Inorg. Chem.*, 2008, **29**, 93–127.

35. R. J. Charlton, C. M. Harris, H. Patil, and N. C. Stephenson, *Inorg. Nucl. Chem. Lett.*, 1966, **2**, 409–414.

36. S. M. Drew, D. E. Janzen, C. E. Buss, D. I. MacEwan, K. M. Dublin, and K. R. Mann, *J. Am. Chem. Soc.*, 2001, **123**, 8414–8415.

37. P. Braunstein and R. J. H. Clark, *J. Chem. Soc. Dalt. Trans.*, 1973, 1845–1848.

38. M. I. Kahn, J. A. Golen, A. L. Rheingold, and L. H. Doerrer, *Acta Cryst.*, 2009, **65**, m1135.

39. A. Bondi, *J. Phys. Chem.*, 1966, **70**, 3006–3007.

40. A. Bondi, *J. Phys. Chem.*, 1964, **68**, 441–451.

41. S. S. Batsanov, *Russ. J. Inorg. Chem.*, 1991, **36**, 3015–3037.

42. N. L. Allinger, X. Zhou, and J. Bergsma, *J. Mol. Struct. THEOCHEM*, 1994, **312**, 69–83.

43. S. S. Batsanov, *J. Mol. Struct.*, 1999, **468**, 151–159.

44. S. S. Batsanov, *Russ. J. Phys. Chem.*, 2000, **74**, 1273–1276.

45. Y. V. Zefirov, *Russ. J. Inorg. Chem.*, 2000, **45**, 1552–1554.

46. S. S. Batsanov, *Inorg. Mater.*, 2001, **37**, 871–885.

47. S. Z. Hu, Z. H. Zhou, and K. R. Tsai, *Acta Phys.-Chim. Sin.*, 2003, **19**, 1073–1077.

48. S. Nag, K. Banerjee, and D. Datta, *New J. Chem.*, 2007, **31**, 832–834.

49. S.-Z. Hu, Z.-H. Zhou, and B. E. Robertson, *Z. Krist.*, 2009, **224**, 375–383.

50. S. Alvarez, *Dalton. Trans.*, 2013, **42**, 8617–8636.

51. D. M. P. Mingos and A. L. Rohl, *Dalton. Trans.*, 1991, 3419–3425.

52. J. Muñiz, C. Wang, and P. Pyykkö, *Chem. Eur. J.*, 2011, **17**, 368–377.

53. R. F. W. Bader, *Atoms in Molecules: A Quantum Theory*, Clarendon Press, Oxford, 1990.

54. P. Politzer and J. S. Murray, *ChemPhysChem*, 2013, **14**, 278–294.

55. Bruker AXS, *APEX2 - Software Suite for Crystallographic Programs*, Bruker AXS, Inc., Madison, WI, USA, 2009.

56. Bruker AXS, *SAINT*, Bruker AXS, Inc.: Madison, WI, USA, 2009.

57. Z. Otwinowski, W.; Minor, in *Methods in Enzymology, Macromolecular Crystallography, Part A*, eds. C. W. Carter and J. Sweet, Academic Press, New York, USA, 1997, pp. 307–326.

58. G. M. Sheldrick, *Acta Crystallogr. A.*, 2008, **64**, 112–122.

59. L. Palatinus and G. Chapuis, *J. Appl. Crystallogr.*, 2007, **40**, 786–790.

60. O. V. Dolomanov, L. J. Bourhis, R. J. Gildea, J. A. K. Howard, and H. Puschmann, *J. Appl. Crystallogr.*, 2009, **42**, 339–341.

61. G. M. Sheldrick, *SADABS - Bruker AXS scaling and absorption correction*, Bruker AXS, Inc., Madison, Wisconsin, USA, 2008, 2008.

62. G. M. Sheldrick, *SHELXTL*, Bruker AXS, Inc., Madison, Wisconsin, USA, 2008.

63. M. J. Frisch, G. W. Trucks, H. B. Schlegel, G. E. Scuseria, M. A. Robb, J. R. Cheeseman, G. Scalmani, V. Barone, B. Mennucci, G. A. Petersson, H. Nakatsuji, M. Caricato, X. Li, H. P. Hratchian, A. F. Izmaylov, J. Bloino, G. Zheng, J. Sonnenb, and D. J. Fox, *Gaussian 09, Revision C.01*, Gaussian, Inc., Wallingford CT, 2009.

64. J. P. Perdew, K. Burke, and M. Ernzerhof, *Phys. Rev. Lett.*, 1996, **77**, 3865–3868.

65. D. Andrae, U. Häußermann, M. Dolg, H. Stoll, and H. Preuß, *Theor. Chim. Acta*, 1990, **77**, 123–141.

66. T. A. Keith, *AIMAll (Version 12.06.03)*, TK Gristmill Software, Overland Park KS, USA, 2012 (aim.tkgristmill.com).